RSC Advances

ROYAL SOCIETY OF CHEMISTRY

www.rsc.org/advances

Graphical Abstract

High-dispersive FeS_2 on graphene oxide for effective degradation of 4-chlorophenol

Graphical abstract: High-dispersive FeS_2 particles on graphene oxide (FeS_2@GO) was prepared by a one-pot hydrothermal method for efficient removal and mineralization of aqueous 4-chlorophenol (4-CP) under slightly acidic or alkaline conditions.

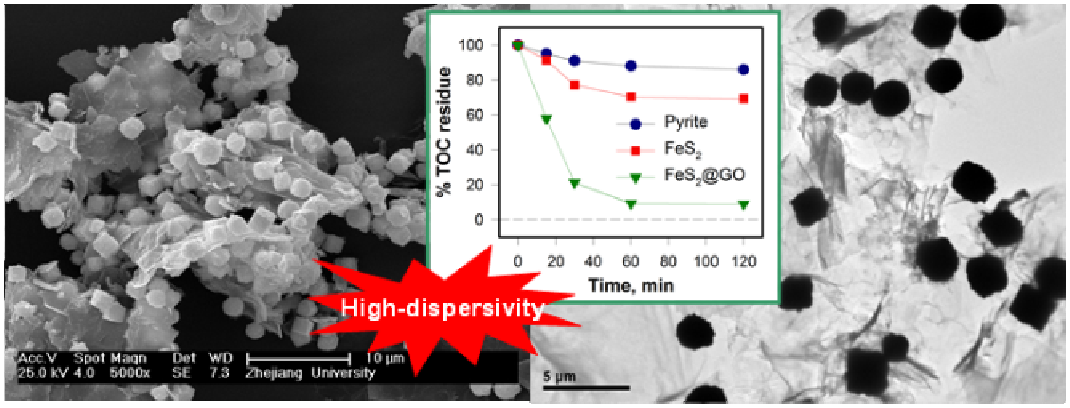

High-dispersive FeS_2 on graphene oxide for effective degradation of 4-chlorophenol

Wanpeng Liu [a], Lili Xu [a], Xingfa Li [a], Chensi Shen [b], Sadia Rashid [b], Yuezhong Wen[a,*], Weiping Liu [a], Xiaohua Wu [c]

[a] *Institute of Environmental Science, College of Environmental and Resource Sciences, Zhejiang University, Hangzhou 310058, China*

[b] *College of Environmental Science and Engineering, Donghua University, Shanghai 201620, China*

[c] *College of Chemistry and Life Science, Zhejiang Normal University, Jinhua 310024, China*

[*] Corresponding author: Tel.: +86-571-8898-2421; Fax: +86-571-8898-2421. E-mail address: wenyuezhong@zju.edu.cn (Y.Z. Wen).

ABSTRACT

A high-dispersive FeS_2 micro-cube crystal on graphene oxide (FeS_2@GO) was fabricated by a one-pot hydrothermal method. The catalytic degradation of 4-chlorophenol (4-CP) and its mechanism in FeS_2@GO-based Fenton system was investigated. Under acidic to slight alkaline conditions, FeS_2@GO demonstrated an excellent capacity to remove 4-CP. More than 97% of 4-CP was eliminated within 60 min in pH 7.0 reaction solutions initially containing 0.2 g/L FeS_2@GO, 128.6 mg/L 4-CP and 100 mM H_2O_2 at 25 ± 1 °C, and the removal of 4-CP was further enhanced with increasing FeS_2@GO loadings. In the meantime, the FeS_2@GO also achieved a lower iron leaching and a more complete TOC removal compared with pure synthetic FeS_2 without graphene oxide. Furthermore, acetic acid and oxalic acid were identified as the primary products. The remarkable capacity of the FeS_2@GO-based Fenton system in removing 4-CP displays its potential application in the treatment of organic compound-contaminated water.

Introduction

Pyrite (FeS_2) is one of the most abundant metal sulfide minerals on the Earth, possessing the degradation capacity of contaminants[1]. For example, degradation kinetics and mechanism of aqueous trichloroethylene (TCE) in aerobic pyrite suspensions has been researched with O_2 as the common oxidant[2-4]. Liang et al.[5] investigated oxidative degradation of methyl *tert*-butyl ether (MTBE) by activated persulfate, using pyrite as the source of ferrous ion activators. Recently, pyrite has been considered as a potential and promising heterogeneous iron source for Fenton-like system to treat various environmental organic pollutants in wastewater and groundwater[6-10]. However, for the limitations of pool purity of natural pyrite, its Fenton-like catalytic capacity can't be further improved. It is known that the catalytic activity of catalysts depends on the size distributions and morphologies of the particles[11]. Hence, reducing the diameter of the material to the nanometer or micrometer scale may result in enhanced its efficacy. But, the difficulty in obtaining fine particles because of its high Mons' hardness scale is the other limitation for further improvement in efficiency.

The hydrothermal method was an alternative way for obtaining more pure and small particles. Up to now, FeS_2 nanocrystallines with different morphologies have been synthesized via various solventhermal methods. One-dimensional nanowires of FeS_2 were synthesized in large quantities by solvothermal process at relatively low temperature with different with morphologies by Kar and Chaudhuri[12], and single phase FeS_2 nanocrystals with cubic shapes were synthesized but in a relative complicated solventhermal process[13]. Afterward well-defined FeS_2 micro-cubes and micro-octahedra

with high-yield and good uniformity were synthesized by a more simple polymer-assisted hydrothermal method[14,15]. However, these FeS_2 particles are prone to aggregate and form large particles during the hydrothermal synthesis process, thus losing their dispersibility and specific area which eventually diminish their activity. Therefore, it is necessary to prepare high-dispersive FeS_2 on a suitable support to preserve or even improve their unique properties[16-18].

In the past decade, graphene and its derivatives are widely investigated as promising materials for the immobilization of nanoparticles. However, the lack of surface functionalities in graphene to directly immobilize the nanoparticles onto its surfaces has led to favorable utilization of graphene oxide (GO) as an alternative support for the assembly of graphene based nanocomposites[19]. GO is fabricated by exfoliating of graphite oxide and is abundant of oxygenated functional groups, such as hydroxyl and epoxides on the plane with carbonyl and carboxyl groups at the edges. These oxygenated functional groups can serve as nucleation sites for metal ions to form GO/nanoparticles composites. As a result, GO used as an attractive material in this field owing to its unique two-dimensional lamellar structure, large surface area, and full surface accessibility[20]. The graphene or GO is not only able to prevent the aggregation of immobilized particles but also improve the overall catalytic activity owing to the synergistic effects between both components[21,22]. For example, several recent studies have been reported using GO for the support of Fe_3O_4 NPs in catalysis for the oxidation of cysteine[23] and 3,3,5,5-tetramethylbenzidine[24], and the reduction of nitrobenzene[25]. Furthermore, the reported enhancement in catalytic activity was attributed to the

synergistic effects between GO sheets and Fe_3O_4 nanoparticles.

The objective of the present work was to explore the degradation of 4-CP with FeS_2@GO by investigating removal efficacy and influencing factors such as FeS_2@GO loading, solution pH, and H_2O_2 concentration. The proposed mechanism was given and the principal reaction intermediates were also identified.

Experimental

1. Chemicals

The 4-chlorophenol (4-CP) standard (purity > 99%) was purchased from Aladdin Chemistry (Shanghai, China). Graphene oxide (purity > 99%, single layer ratio > 99%, diameter 1 ~ 5 *μm*, thickness 0.8 ~ 1.2 nm) was purchased from XFNano Inc. (Nanjing, China). Pyrite (purity 95%) was purchased from Strem Chemicals (Newburyport, MA, USA). Triton™ X-100 (TX-100), sulfur (purity 99.5% ~ 100.5%) and 2,9-dimethyl-1,10-phenanthroline (DMP) were purchased from Sigma-Aldrich (St. Louis, MO, USA). Other chemicals and solvents used in this study were of analytical grade or high performance liquid chromatography (HPLC) grade. The concentration of the purchased hydrogen peroxide solution (30 wt%) was calibrated by titration with potassium permanganate[26] and the purchased pyrite was grounded, sieved through 150 *μ*m mesh and washed with 0.1 M HCl prior to use. Other chemicals were used as received. Ultrapure water (18.2 MΩ•cm resistivity) was prepared using a Millipore® purification system and used throughout the experiments. Stock solution of 1.0 M 4-CP was prepared in methanol. The 1% (w/v) DMP solution was prepared in ethanol in a

brown bottle. A 0.01 M copper (II) sulfate ($CuSO_4$) solution was prepared by dissolving $CuSO_4 \cdot 5H_2O$ in ultrapure water. All solutions were stored at 4 °C prior to use.

2. Preparation of FeS_2 and FeS_2@GO

Iron disulfide microcube crystal (FeS_2) was synthesized using $FeSO_4$ and sulfur in alkaline solution based on Wang's method[14]. Briefly, 16 mL of non-ionic surfactant TX-100 was added in 44 mL of ethylene glycol (EG) at room temperature followed by addition of 0.39 g of ferrous sulfate heptahydrate ($FeSO_4 \cdot 7H_2O$), forming a homogenous solution under vigorous stirring. Then 0.4 g of sulfur was added to the solution under magnetic stirring for 1 h, after complete dispersion of sulfur powder, 10 mL of 1.5 M NaOH was added and stirred for 30 min. Then the final mixture was sealed in a 100-mL Teflon-lined stainless steel autoclave, and maintained at 180 °C for 12 h, then cooled to room temperature naturally. The resulting black solid was collected by centrifugation, washed alternately with ultrapure water and ethanol several times to remove the excess surfactant and finally dried in vacuum at 50 °C for 10 h before further use. Iron disulfide-graphene oxide composite (FeS_2@GO) was synthesized according to the above procedures with appropriate amount of GO (0.03, 0.06, 0.12 g) dispersed in EG by ultrasonication in advance.

3. Reaction setup

All degradation experiments of 4-CP were carried out in 50-mL glass flasks with a total solution volume of 40 mL under magnetic stirring (400 r/min) and 25 ± 1 °C. A 500-W xenon lamp (Trustech Inc., Beijing, China) was used as the light source for the experiments conducted in the presence of visible light. The light radiates to the solutions

through a glass slide to obtain visible light without UV wave band. The initial pH (pH_i) of the solutions was adjusted to the designated value with 1 M H_2SO_4 and 1 M NaOH standard solution. A 40 μL aliquot of 1.0 M 4-CP stock solution was added to make a nominal initial concentration of 1.0 mM (128.6 mg/L) and appropriate volume of H_2O_2 solution was injected to make a demanded concentration. Reactions were initiated by adding a predetermined amount of pyrite, FeS_2 or FeS_2@GO into the pre-equilibrated and constantly stirred solutions. Aliquots of 1.0 mL sample were periodically withdrawn and filtrated through 0.45 μm syringe filter. The supernatant was transferred to 2-mL vials containing 10 μL of *tert*-butanol (as a radical scavenger) and subjected to HPLC analysis to determine the remaining 4-CP concentration and the formation of carbonyl acids. For the runs of cyclic reaction, the post-reaction FeS_2@GO was collected by filtration and dried in 50°C. For TOC measurement, aliquots of 5 mL sample were periodically withdrawn and filtrated through 0.45 μm syringe filter, but no radical scavenger was added to avoid background TOC interference. All samples were stored at 4 °C and analyzed within 24 h.

To quantify the consumption of H_2O_2 and leaching of Fe ions in the reaction systems, an additional reaction solution without 4-CP was also prepared. For H_2O_2 consumption quantification, 100 μL samples were periodically withdrawn and filtrated through 0.45 μm syringe filter. Aliquots of 50 μL supernatant was transferred to 5-mL volumetric flask and diluted to 500 μL. The dilution was used for H_2O_2 measurement using a method according to Kasaka et al.[27]. The determination of H_2O_2 is based on a spectrophotometric method via the stoichiometric reaction of H_2O_2 with copper (II) ion

and DMP. Briefly, 0.5 mL each of DMP, $CuSO_4$ and phosphate buffer was added to a 5-mL volumetric flask containing 0.5 mL diluted sample supernatant and the flask was filled up to 5 mL with water. After mixing, the solution was transferred to 1-cm cells and the absorbance was measured at 454 nm on a Shimadzu UV-2401 PC UV/Vis spectrophotometer (Tokyo, Japan). While, for Fe ions leaching quantification, aliquots 2 mL sample were withdrawn and filtrated through 0.45 μm syringe filter. The supernatant was transferred to 5-mL vials containing 10 μL HNO_3 (65 wt%) and subjected to inductively coupled plasma mass spectrometry (ICP-MS) analysis to determine the Fe ions concentration.

4. Chemical analysis

The 4-chlorophenol and by-products concentrations in reaction samples were determined using a Waters® 2695 reverse-phase HPLC coupled with a Waters® 2998 photodiode array detector (Milford, MA, USA). The detection wavelength was both 210 nm. A Waters® XBridge™ Phenyl column (250 × 4.6 mm, 5 μm) was employed for the separation of 4-chlorophenol. The isocratic mobile phase consisted of 70% methanol and 30% water with a flow rate of 0.8 mL/min. The injection volume was 20 μL. Under these conditions, the typical retention time for 4-CP was 5.5 min. For the products such as carbonyl acids, a Waters® Atlantis™ T3 column (250 × 4.6 mm, 5 μm) was employed for the separation. The isocratic mobile phase was 10 mM NaH_2PO_4 aqueous solution (adjusting pH to 3.0 with H_3PO_4) with a flow rate of 0.5 mL/min. The injection volume was 50 μL. Under these conditions, the typical retention time for acetic acid, oxalic acid and chloroacetic were 6.1, 12.7 and 14.1 min, respectively.

5. Characterization

Surface morphology studies of FeS_2 and FeS_2@GO were achieved with a field emission scanning electron microscope (FEI, SIRON) at a voltage of 25.0 kV to test. The sample surfaces were gold-coated before analysis. The microstructures were further examined by transmission electron microscopy (TEM, JEM1200EX, JEOL). X-ray diffraction (XRD) measurements were conducted using a D8 Advance (Bruker, Germany) X-ray diffractometer with Cu Ka radiation (λ = 1.5418 Å).

Results and discussion

1. Characterization of FeS_2 and FeS_2@GO

The morphology and microstructures of synthetic FeS_2 and FeS_2@GO were investigated by a scanning electron microscope (SEM). Fig. 1a and Fig. 1b showed the SEM images of FeS_2 and FeS_2@GO, respectively. It illustrates that the shape of synthetic FeS_2 is irregular, and it is unhomologous in size. Besides, the FeS_2 crystal aggregates as clusters, making an obscure microcube structure and a low surface area (3.48 m^2/g). On the other hand, GO facilitates the dispersion of FeS_2 during the synthesis process. The FeS_2 synthesized with GO sheets spiking was found to be single crystal with distinct microcubic structures. It is also homologous in size (800 ~ 1000 nm), which has a much larger surface area (23.26 m^2/g) compared with FeS_2 synthesized without GO. The microstructures of FeS_2 and FeS_2@GO were further examined by transmission electron microscopy (TEM) images (Fig. 1c and Fig. 1d) and

drawn a same result. Furthermore, the composition and phase purity of natural pyrite and synthetic FeS_2 were examed by XRD (Fig. 2). It can be seen that all reflection peaks in the red line can be readily indexed as a pure cubic phase of FeS_2, which is consistent with value given in Joint Committee on Powder Diffraction Standards (JCPDS) diffraction data files (No. 71-2219). However, a lower purity of pyrite can be easily observed in the black line with relatively poor clearness in reflection peaks.

2. Removal of 4-chlorophenol by FeS_2@GO

A typical degradation profile of 4-CP by FeS_2 and FeS_2@GO is given in Fig. 3a. For verifying and comparing the capacity of iron disulfide in organics removal, commercially available natural pyrite crystals (the major ingredient is iron disulfide) were also employed for the removal of 4-CP. According to the results, FeS_2@GO possesses a fairly high capacity in removing 4-CP in H_2O_2 solutions compared to FeS_2 particles and pyrite, both the synthesis and none-synthesis iron disulfide. For example, 86% of 4-CP was removed in 30 min in a pH 5.0 reaction system originally containing 0.8 g/L FeS_2@GO, 50 mM H_2O_2 and 1.0 mM 4-CP, while only 58% and 19% 4-CP was removed by FeS_2 and pyrite under the same conditions, respectively. Up to 99% of 4-CP disappeared as the reaction was prolonged to 60 min as well as 97% for FeS_2. However, the inevitable aggregation of FeS_2 during the reaction tends to inhibit the removal rate and can't be ignored. As a result, natural pyrite have the lowest efficiency for 4-CP removal as compared to FeS_2 and FeS_2@GO. And FeS_2@GO possesses the most remarkable dispersibility as well as 4-CP removal efficiency in the reaction process. To study the effect of GO content on the efficiency of FeS_2@GO for removal of 4-CP and

fix an appropriate GO amount during the synthesis process, FeS_2@GO with different GO content was employed for 4-CP removal. As shown in Fig. 3b, efficacy of 4-CP removal by FeS_2@GO in H_2O_2 solutions was slightly improved as the GO content of FeS_2@GO increased. Take both economy and efficiency into consideration, 0.03 g was chosen as the optimal amount for spiking in FeS_2@GO synthesis, and was employed throughout all experiments below.

3. Leaching of iron

The level on the iron leaching is another essential factor to evaluate the Fenton-like catalytic performance. The aqueous iron content in the FeS_2-H_2O_2 or FeS_2@GO-H_2O_2 suspension was detected by inductively coupled plasma mass spectrometry (ICP-MS) during a 2-h reaction. According to the results, the leaching rate of FeS_2 was a little faster than that of FeS_2@GO (Fig. 4a). For example, after 120 min reaction, the concentration of aqueous iron was 5.4 mg/L for FeS_2, while it was 4.5 mg/L for FeS_2@GO, equaling to only 0.81% and 0.68% of the initial iron content. Meanwhile, the total iron content in FeS_2@GO was 98.9% of that in FeS_2. It is reported that the charges on GO surface are highly negative when dispersed in water attribute to the ionization of the carboxylic acid and the phenolic hydroxyl groups[28]. Hence, the most plausible reason was that Fe^{3+}/Fe^{2+} was adsorbed on the GO surface through static interaction or complex with oxygenated functional groups[29]. But the leaching iron makes fairly finite contribution to 4-CP removal. As shown in Fig. 4b, only 42% of 4-CP was eliminated within 60 min in a Fenton system with 5.4 mg/L Fe^{2+} and 50 mM H_2O_2.

4. Effect of FeS_2@GO loading, pH and H_2O_2 concentration

The removal rate of 4-CP increased with the initial FeS_2@GO content (Fig. 5a). For example, 4-CP removal at 60 min increased from 76% for a solution with 0.2 g/L FeS_2@GO to 100% with 0.8 g/L FeS_2@GO. Two factors are responsible for the enhanced removal of 4-CP with increasing loading. It is reported by Bae et al.[7] the hydroxyl radicals (•OH), which are the dominantly oxidant for the decomposition of organic compounds in pyrite Fenton reaction, were generated through reduction of H_2O_2 by Fe^{2+} dissolved from FeS_2 under aerobic condition (Eq. (1)).

$$2FeS_2 + 7O_2 + 2H_2O \rightarrow 2Fe^{2+} + 4SO_4^{2-} + 4H^+ \quad (1)$$

The removal of 4-CP in the FeS_2@GO-based Fenton system was obviously pH-dependent. Overall, 4-CP removal rates decreased with increasing pH_i (Fig. 5b), suggesting that acidic conditions facilitated 4-CP removal. For example, 4-CP removal rate at 30 min decreased from 86% for the reaction solution with pH_i 5.0 to 59% for that with pH_i 9.0. When pH_i was increased to 11.0, 4-CP removal rate was inhibited to a relatively low value of 21%, which is attribute to the decreasing formation of •OH caused by low Fe^{2+} concentration at high pH[1]. Similarly, pH was a major factor that affected the removal of other organics (e.g. trichloroethylene and 2,4,6-trinitrotoluene) in pyrite Fenton systems[7,8]. However, it is well known that in a classic Fenton system aqueous Fe(II) leading to decomposition of H_2O_2 to hydroxyl radicals was only efficiently occurred at the pH below 4.5[30]. In the present work, the FeS_2@GO-mediated removal of 4-CP stayed in a high rate in a slight acidic to alkaline conditions (pH 5.0 ~ 9.0), even in a strong alkaline solution (pH 11.0), 49% of 4-CP was removed in 60 min

yet. As reported by Bonnissel-Gissinger[1], pyrite suspension pH declined and reached an acidic equilibrium point during the oxidation by releasing iron and hydrogen, providing an appropriate pH for the subsequent Fenton reaction. Additionally, the presence of H_2O_2 extremely exacerbated pH decreasing, since pyrite dissolution kinetics by H_2O_2 is much faster than that by molecular oxygen in suspensions[31,32], which leaded to a relatively high removal efficiency for 4-CP under weak acidic to weak alkaline conditions (pH 5.0 ~ pH 9.0). The similar result was observed by Che et al.[7] and Bae et al.[9] in the removal of trichloroethylene and diclofenac, respectively, by pyrite-based Fenton's reaction. Furthermore, the numerous carboxyl groups (−COOH) and hydroxyl groups (−OH) on GO surface also provided an acidic interface for the occurrence of Fenton's reaction[33].

It is well know that in a Fenton system H_2O_2 simultaneously plays as the roles of both of OH• producer (Eq. (2)) and OH• scavenger (Eq. (3))[34,35]. Therefore, the concentration of H_2O_2 is a crucial parameter for 4-CP removal in FeS_2@GO Fenton system.

$$H_2O_2 + Fe^{2+} \rightarrow Fe^{3+} + OH^- + HO\bullet \quad (2)$$

$$H_2O_2 + OH\bullet \rightarrow OH_2\bullet + H_2O \quad (3)$$

As Fig. 5c showed that the removal of 4-CP was increased with the increasing concentration of H_2O_2 in the FeS_2@GO Fenton system. The 4-CP removal rates declined as the concentration of H_2O_2 varies from 12 ~ 50 mM. For example, 4-CP removal rate at 30 min decreased from 17% at the H_2O_2 concentration of 12 mM to 56% and 86% at that of 25 mM and 50 mM, respectively. With the reaction proceeding to 60

min, 4-CP removal rate was respectively increased to 39%, 93% and 100% for H_2O_2 concentrations of 12 mM, 25 mM and 50 mM. As McKibben and Barnes[31] reported, the general mechanism of Fe^{2+} dissolution from the pyrite surface in an aerobic H_2O_2 solution includes two different pathways (Eq. (1) and Eq. (4) and (5)) and the second pathway with two consecutive reactions is considered as the dominant way for Fe^{2+} generation.

$$2FeS_2 + 15H_2O_2 \rightarrow 2Fe^{3+} + 4SO_4^{2-} + 2H^+ + 14H_2O \quad (4)$$

$$FeS_2 + 14Fe^{3+} + 8H_2O \rightarrow 15Fe^{2+} + 2SO_4^{2-} + 16H^+ \quad (5)$$

Therefore, the increasing of H_2O_2 concentration accelerates the 4-CP removal in the FeS_2@GO Fenton system. However, the self scavenging of HO• caused by H_2O_2 concentration increasing seemed to be more significant during the reaction. As a result, further addition of H_2O_2 to 200 mM did not significantly affect 4-CP removal rates (data was not shown) and H_2O_2 concentration was fixed at an optimal level in the following experiments.

5. The reuse of FeS_2@GO

The reuse and stability were two major concerns for a catalyst to be used in practical applications [36-38]. In the durability test, the same FeS_2@GO samples were repeatedly employed for 4-CP removal for consecutive five times. It showed that there were no obvious attenuation in the extent of 4-CP removal was observed (Fig. 6). However, a slight decline inevitably occurred for the loss of catalyst during the reaction and recovery procedures. For example, the removal rate of 4-CP was over 99% for the initial reaction, but it slightly dropped to about 95% for the fifth cycling. It is worth noticing

that the recovery of FeS_2@GO is difficult for its high dispersibility in the reaction solutions. Therefore, further research would still need to be conducted to generate enhanced separation properties for FeS_2@GO.

6. Identified products

It is well known that organic compounds were expected to oxidize to short-chain carboxylic acids (e.g., formic acid, acetic acid, oxalic acid and maleic acid) and then finally minerals, CO_2 and H_2O [39]. In this study, three carboxylic acids including oxalic acid, acetic acid and chloroacetic acid were identified as the primary intermediates through HPLC-DAD analysis and the time profile of the intermediates were given in Fig. 7. It is shown that oxalic acid and acetic acid accumulated in the early stage, and then attenuated after reaching a peak value. For example, oxalic acid accumulated to a peak concentration of 0.35 mM at 5 min and then declined, no oxalic acid was detected after 30 min. Similarly, acetic acid accumulated to a peak concentration of 0.89 mM at 30 min and was not detected after 60 min. However, the same course was not observed on chloroacetic acid. It kept on a relative low level compared with oxalic acid and acetic acid. To investigate the mineralization of 4-CP, concentrations of TOC were measured during the oxidative degradation of 4-CP by FeS_2@GO Fenton system. It is shown in Fig. 8 that after 60 min reaction 91%, 70% and 12% of TOC was removed for FeS_2@GO, FeS_2 and pyrite, respectively.

7. Proposed mechanism

Previous study has proved that FeS_2 has a higher optical absorption coefficient than silicon but has a comparable band gap energy (E_g = 0.95 eV)[40]. Additionally, single

layered GO have a high optical transmittance, especially for visible light[41]. In our experiments, the removal process of 4-CP was exposed to indoor natural light, so we conducted a control experiment in the dark. As a result, no obvious diversity on 4-CP removal was observed under natural light and dark condition, indicating that FeS_2@GO-H_2O_2 system also works well in dark. Furthermore, for the photo-oxidation efficiency of photocatalysts was found to generally depend on light intensity[42], the intense light source xenon lamp with a UV-light filter was employed in the experiment for 4-CP removal. Similarly, the concentration of 4-CP declined the same as in dark (Fig. 9). Therefore, it is considered that the FeS_2@GO-H_2O_2 system without the photo-catalytic process would avoid the drawbacks found in light sensitive system.

According to the previous studies[4, 7, 8, 10], the Fenton reaction stimulated by the dissolved Fe^{2+} from pyrite surface is the dominant mechanism for 4-CP removal. Overall, H_2O_2 consumption rates in different reaction systems followed the order of pyrite > FeS_2@GO > FeS_2 (Fig. 10), because GO highly facilitated dispersion of FeS_2 and provided a huge interface for the transformation of H_2O_2, enhancing the 4-CP removal.

The role of H_2O_2 in the removal of 4-CP was precursor of HO•. Because H_2O_2 itself is not an efficient oxidizer of 4-CP, HO• generated from H_2O_2 are the actual oxidant in the FeS_2 and FeS_2@GO Fenton systems. It is showed in Fig. 11 that addition of methanol as a HO• scavenger substantially retarded the removal of 4-CP both in FeS_2 and FeS_2@GO Fenton systems. Besides, it is worth to notice that in an anaerobic reaction system 4-CP removal was also inhibited to a certain degree (Fig. 11). Thus, it is

believed oxygen played an indispensable role in the FeS_2@GO Fenton system for 4-CP removal. First, it is proved that the transformation of halogenated compounds in pyrite suspension was consistent with the finding that pyrite oxidation by O_2 follows a Fenton-like mechanism, in which the reduction of O_2 on the pyrite surface can induce HO• formation[43-48]. On the other hand, the dissolved O_2 in reaction solutions oxide the FeS_2@GO surface, releasing Fe^{2+} for the further Fenton reaction (Eq. (3)). Therefore, dissolved O_2 is an essential factor in the FeS_2@GO Fenton system. In addition, it is considered that the surface disulfide groups have been the proposed electron donor in reductive dehalogenation[49].

Conclusions

This study demonstrated that high-dispersive FeS_2 on GO possesses a relatively high oxidative capacity for removing aqueous 4-CP in H_2O_2 solution, offering a good alternative for the treatment of aqueous organic contaminants. The continuous dissolution of Fe^{2+} from FeS_2@GO surface is considered as the key factor to achieve the oxidation of 4-CP by continuously producing the •OH. And oxygen played an indispensable role in the FeS_2@GO Fenton system for 4-CP removal by facilitating the dissolution of Fe^{2+}. Besides, no distinguishable diversity on removal of 4-CP was observed in presence and absence of visible light. The results obtained from this study can provide basic knowledge to understand the oxidative degradation mechanism of 4-CP by high-dispersive FeS_2 in H_2O_2 solution and to design a high-dispersive and efficient heterogeneous Fenton catalyst for treatment of organic-contaminated water.

Acknowledgements

The authors acknowledge financial support from "The Opening Foundation of the Environmental Engineering Key Discipline", the Fundamental Research Funds for the Central Universities and the Zhejiang Provincial Natural Science Foundation of China (No. LY12B050005).

Notes and references

1 P. Bonnissel-Gissinger, M. Alnot, J. J. Ehrhardt and P. Behra, *Environ. Sci. Technol.*, 1998, **32**, 2839-2845.

2 H. T. Pham, M. Kitsuneduka, J. Hara, K. Suto and C. Inoue, *Environ. Sci. Technol.*, 2008, **42**, 7470-7475.

3 H. T. Pham, K. Suto and C. Inoue, *Environ. Sci. Technol.*, 2009, **43**, 6744-6749.

4 R. Weerasooriya and B. Dharmasena, *Chemosphere*, 2001, **42**, 389-396.

5 C. J. Liang, Y. Y. Guo, Y. C. Chien and Y. J. Wu, *Ind. Eng. Chem. Res.*, 2010, **49**, 8858-8864.

6 M. Arienzo, *Chemosphere*, 1999, **39**, 1629-1638.

7 H. Che, S. Bae and W. Lee, *J. Hazard. Mater.*, 2010, **185**, 1355-1361.

8 R. Matta, K. Hanna and S. Chiron, *Sci. Total Environ.*, 2007, **385**, 242-251.

9 S. Bae, D. Kim and W. Lee, *Appl. Catal. B: Environ.*, 2013, **134**, 93-102.

10 H. Che and W. Lee, *Chemosphere*, 2011, 82, 1103-1108.

11 L. L. Xu, X. F. Li, J. Q. Ma, Y. Z. Wen and W. P. Liu, *Appl. Catal. A: Gen.*, 2014, **485**, 91-98.

12 S. Kar and S. Chaudhuri, *Chem. Phys. Lett.*,2004, **398**, 22-26.

13 C. Wadia, Y. Wu, S. Gul, S. K. Volkman, J. H. Guo and A. P. Alivisatos, *Chem. Mater.*,2009, **21**, 2568-2570.

14 D. W. Wang, Q. H. Wang and T. M. Wang, *CrystEngComm*, 2010, **12**, 755-761.

15 D. W. Wang, Q. H. Wang and T. M. Wang, *CrystEngComm*, 2010, **12**, 3797-3805.

16 S. Q. Song, R. C. Rao, H. X. Yang, H. D. Liu and A. M. Zhang, *Nanotechnology*, 2010, **21**, 185602-185607.

17 D. N. Thi, H. P. Ngoc, H. D. Manh and T. N. Kim, *J. Hazard. Mater.*, 2011, **185**, 653-661.

18 A. Prakash, S. Chandra and D. Bahadur, *Carbon*, 2012, **50**, 4209-4219.

19 H. X. Wu, G. Gao, X. J. Zhou, Y. Zhang and S. W. Guo, *CrystEngComm*, 2012, **14**, 499-504.

20 W. Fan, W. Gao, C. Zhang, W. W. Tjiu, J. S. Pan and T. X. Liu, *J. Mater. Chem.*, 2012, **22**, 25108-25115.

21 Y. Choi, H. S. Bae, E. Seo, S. Jang, K. H. Park and B. S. Kim, *J. Mater. Chem.*, 2011, **21**, 15431-15436.

22 T. Zeng, X. L. Zhang, Y. R. Ma, H. Y. Niu and Y. Q. Cai, *J. Mater. Chem.*, 2012, **22**, 18658-18663.

23 Y. H. Song, Z. F. He, H. Q. Hou, X. L. Wang and L. Wang, *Electrochim. Ac.*, 2012, **71**, 58-65.

24 Y. L. Dong, H. G. Zhang, Z. U. Rahman, L. Su, X. J. Chen, J. Hu and X. G. Chen, *Nanoscale*, 2012, **4**, 3969-3976.

25 G. Y. He, W. F. Liu, X. Q. Sun, Q. Chen, X. Wang and H. Q. Chen, *Mater. Res. Bull.*, 2013, **48**, 1885-1890.

26 H. Bader, V. Sturzenegger and J. Hoigné, *Water Res.*, 1988, **22**, 1109-1115.

27 K. Kasaka, H. Yamada, S. Matsui, S. Echigo and K. Shishida, *Environ. Sci. Technol.*, 1998, **32**, 3821-3824.

28 D. Li, M. B. Muller, S. Gilje, R. B. Kaner and G. G. Wallace, *Nat. Nanotechnol.*, 2008, **3**, 101-105.

29 N. A. Zubir, C. Yacou, J. Motuzas, X. W. Zhang and J. C. D. da Costa, *Sci. Rep.*, 2014, **4**, 1-8.

30 S. Navalon, M. Alvaro and H. Garcia, *Appl. Catal. B: Environ.*, 2010, **99**, 1-26.

31 M. A. McKibben and H. L. Barnes, *Geochim. Cosmochim. Ac.*, 1986, **50**, 1509-1520.

32 P. C. Singer and W. Stumm, *Science*, 1970, **167**, 1121-1123.

33 X. M. Ren, J. X. Li, X. L. Tan, W. Q. Shi, C. L. Chen, D. D. Shao, T. Wen, L. F. Wang, G. X. Zhao, G. P. Sheng and X. K. Wang, *Environ. Sci. Technol.*, 2014, **48**, 5493-5500.

34 C. K. Duesterberg and T. D. Waite, *Environ. Sci. Technol.*, 2006, **40**, 4189-4195.

35 X. F. Li, X. Liu, L. L. Xu, Y. Z. Wen, J. Q. Ma, Z. C. Wu, *Appl. Catal. B: Environ.*, 2015, **165**, 79-86.

36 C. S. Shen, Y. Shen, Y. Z. Wen, H. Y. Wang, W. P. Liu, *Water Res.*, 2011, **45**, 5200-5210.

37 C. S. Shen, Y. Z. Wen, X. D. Kang, W. P. Liu, *Chem. Eng. J.*, 2011, **166**, 474-482.

38 C. S. Shen, H. Chen, S. S. Wu, Y. Z. Wen, L. N. Li, Z. Jiang, M. C. Li, W. P. Liu, *J. Harzd. Mater.*, 2013, **244-245**, 689-697.

39 C. S. Shen, Y. Z. Wen, Z. L. Shen, J. Wu, W. P. Liu, *J. Harzd. Mater.*, 2011, **193**, 209-215.

40 S. Ogawa, *J. Appl. Phys.*, 1979, **50**, 2308-2311.

41 V. Singh, D. Joung, L. Zhai, S. Das, S. I. Khondaker and S. Seal, *Prog. Mater. Sci.*, 2011, **56**, 1178-1271.

42 C. S. Shen, S. F. Song, L. L. Zang, X. D. Kang, Y. Z. Wen, W. P. Liu and L. S. Fu, *J. Harzd. Mater.*, 2010, **177**, 560-566.

43 M. Berger, M. Hazen, A. Nejjari, J. Fournier, J. Guignard, H. Pezerat and J. Cadet, *Carcinogenesis*, 1993, **14**, 41-46.

44 C. A. Cohn, M. J. Borda and M. A. A. Schoonen, *Earth Planet. Sci. Lett.*, 2004, **225**, 271-278.

45 C. A. Cohn, R. Laffers and M. A. A. Schoonen, *Environ. Sci. Technol.*, 2006, **40**, 2838-2843.

46 C. A. Cohn, S. Mueller, E. Wimmer, N. Leifer, S. Greenbaum, D. R. Strongin and M. A. A., *Geochem. Trans.*, 2006, **7**, open assess.

47 R. T. Lowson, *Chem. Rev.*, 1982, **82**, 461-497.

48 J. D. Rimstidt and D. J. Vaughan, *Geochim. Cosmochim. Ac.*, 2003, **67**, 873-880.

49 G. W. Luther, *Geochim. Cosmochim. Ac.*, 1987, **51**, 3193-3199.

FIGURE CAPTIONS

Fig. 1 SEM image of FeS_2 (a) and FeS_2@GO (b), and TEM images of FeS_2 (c) and FeS_2@GO (d).

Fig. 2 X-ray diffraction patterns of natural pyrite and synthetic FeS_2.

Fig. 3 Time profiles of 4-chlorophenol (4-CP) removal by pyrite, FeS_2 FeS_2@GO (a), and time profiles of 4-CP removal by FeS_2@GO with different GO content (b) under the conditions of pH 5.0, 25 ± 1 °C, [4-CP] = 128.6 mg/L (1.0 mM), [H_2O_2] = 50 mM and [catalyst] = 0.8 g/L. Data points are given as means ± standard deviations (n = 3).

Fig. 4 Iron leaching of FeS_2 and FeS_2@GO during the reaction with 4-hlorophenol (4-CP) (a) and time profiles of 4-CP in classic Fenton system (b) under the conditions of pH 5.0, 25 ± 1 °C, [4-CP] = 128.6 mg/L (1.0 mM), [H_2O_2] = 50 mM, [catalyst] = 0.8 g/L and [Fe^{2+}] = 5.4 mg/L. Data for classic Fenton treatment are from single measurement, while the other data points are given as means ± standard deviations (n = 3).

Fig. 5 Effect of FeS_2@GO loading (a), initial pH (b) and H_2O_2 concentration (c) on 4-chlorophenol (4-CP) removal at 25 ± 1 °C in pH 5.0 reaction solutions initially containing 128.6 mg/L (1.0 mM) 4-CP and 50 mM H_2O_2 and 0.8 g/L FeS_2@GO. Data for FeS_2@GO-only treatment are from single measurements, whereas the other data

points are given as means ± standard deviations (n = 3).

Fig. 6 Reuse of FeS_2@GO at 25 ± 1 °C in pH 5.0 reaction solutions initially containing 128.6 mg/L (1.0 mM) 4-CP, 50 mM H_2O_2 and 0.8 g/L FeS_2@GO. (a-e) show 4-CP residue in five degradation reactions. Data points are from single measurement.

Fig. 7 Formation of intermediates oxalic acid, acetic acid and chloroacetic acid.

Fig. 8 Removal of TOC at 25 ± 1 °C in pH 5.0 reaction solutions initially containing 128.6 mg/L (1.0 mM) 4-CP, 50 mM H_2O_2 and 0.8 g/L FeS_2@GO (pyrite or FeS_2). Data points are from single measurement.

Fig. 9 Effect of visible light on 4-chlorophenol (4-CP) at 25 ± 1 °C in pH 5.0 reaction solutions initially containing 128.6 mg/L (1.0 mM) 4-CP, 50 mM H_2O_2, and 0.8 g/L FeS_2@GO. Data for visible light treatment are from single measurement, while the other data points are given as means ± standard deviations (n = 3).

Fig. 10 Hydrogen peroxide consumption by pyrite, FeS_2 and FeS_2@GO at 25 ± 1 °C in pH 5.0 reaction solutions initially containing 50 mM H_2O_2 and 0.8 g/L FeS_2@GO (pyrite or FeS_2). Data points are given as means ± standard deviations (n = 3).

Fig. 11 Removal of 4-chlorophenol (4-CP) at 25 ± 1 °C in pH 5.0 reaction solutions in

the presence of 2.5% wt. methanol (•OH radical scavenger) and in the absent of O_2 initially containing 128.6 mg/L 4-CP, 50 mM H_2O_2 and 0.8 g/L FeS_2@GO (or FeS_2). Data for anaerobic treatment are from single measurement, while the other data points are given as means ± standard deviations (n = 3).

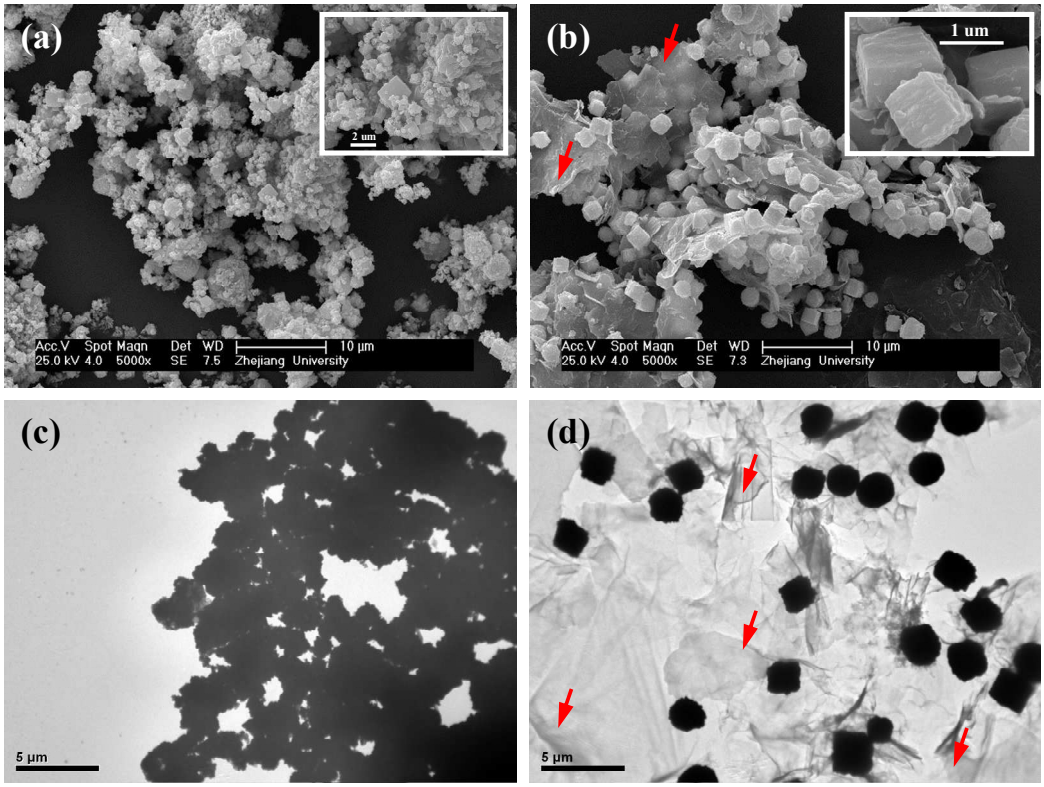

Fig. 1

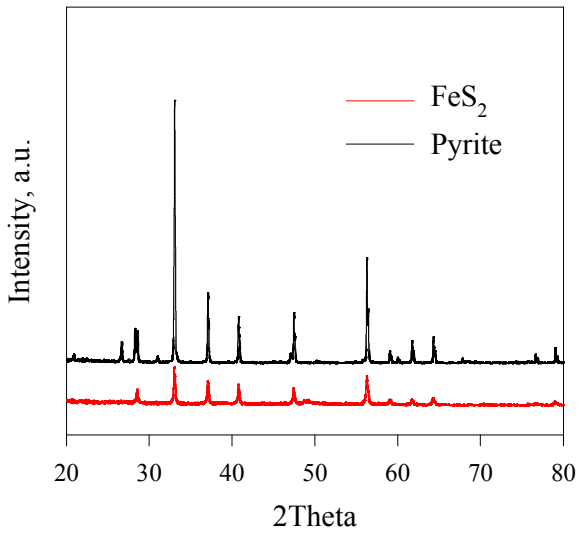

Fig. 2

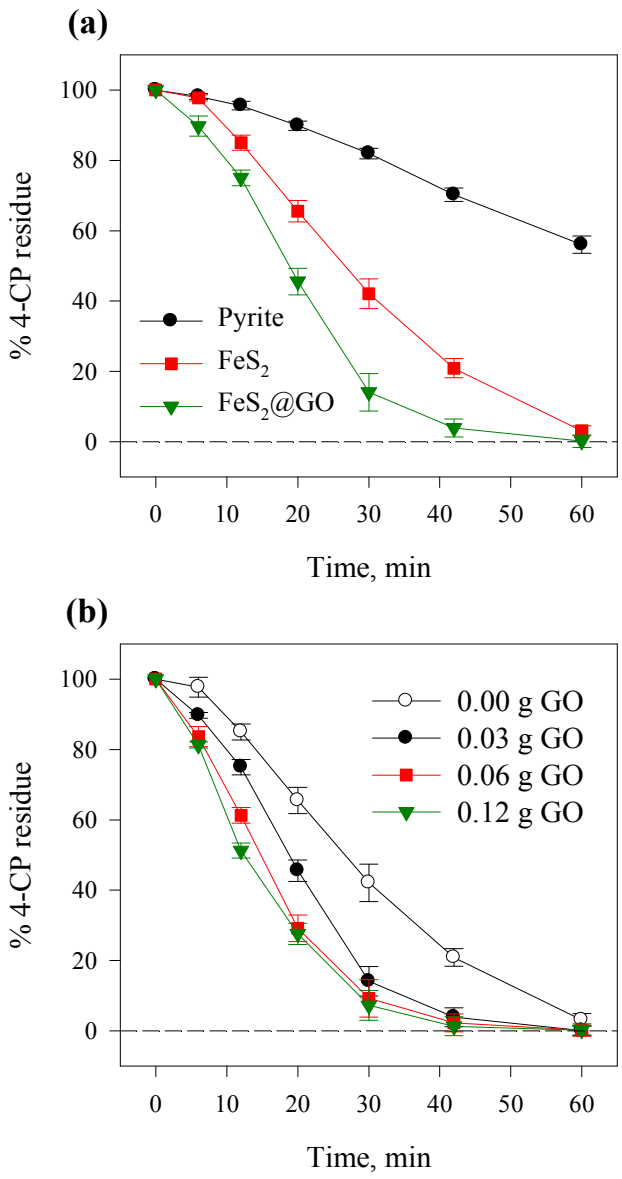

Fig. 3

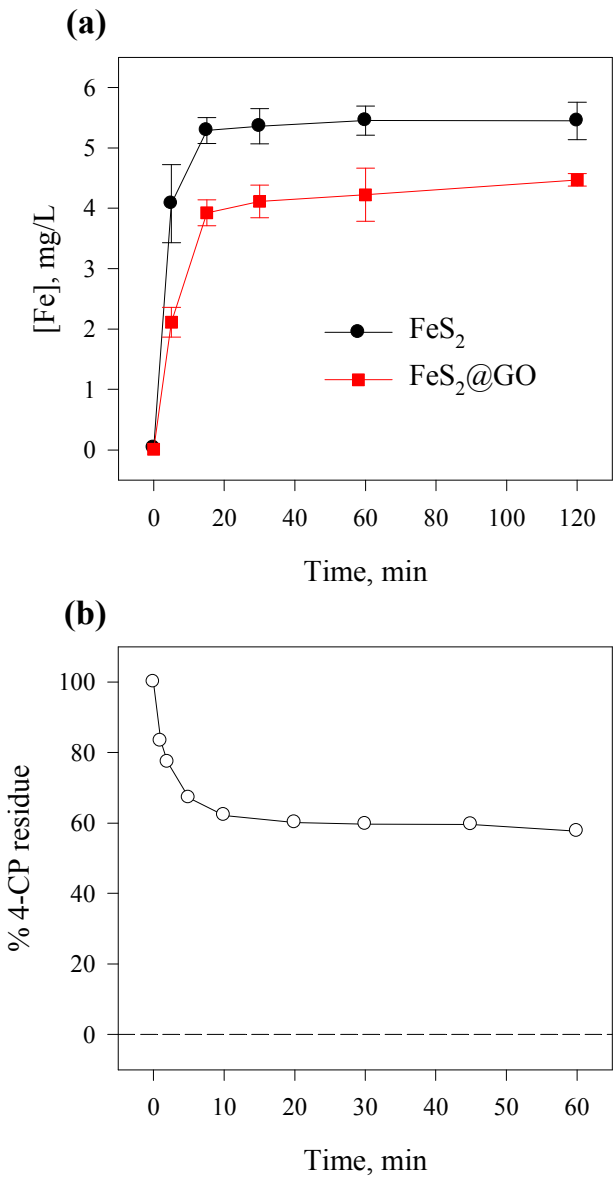

Fig. 4

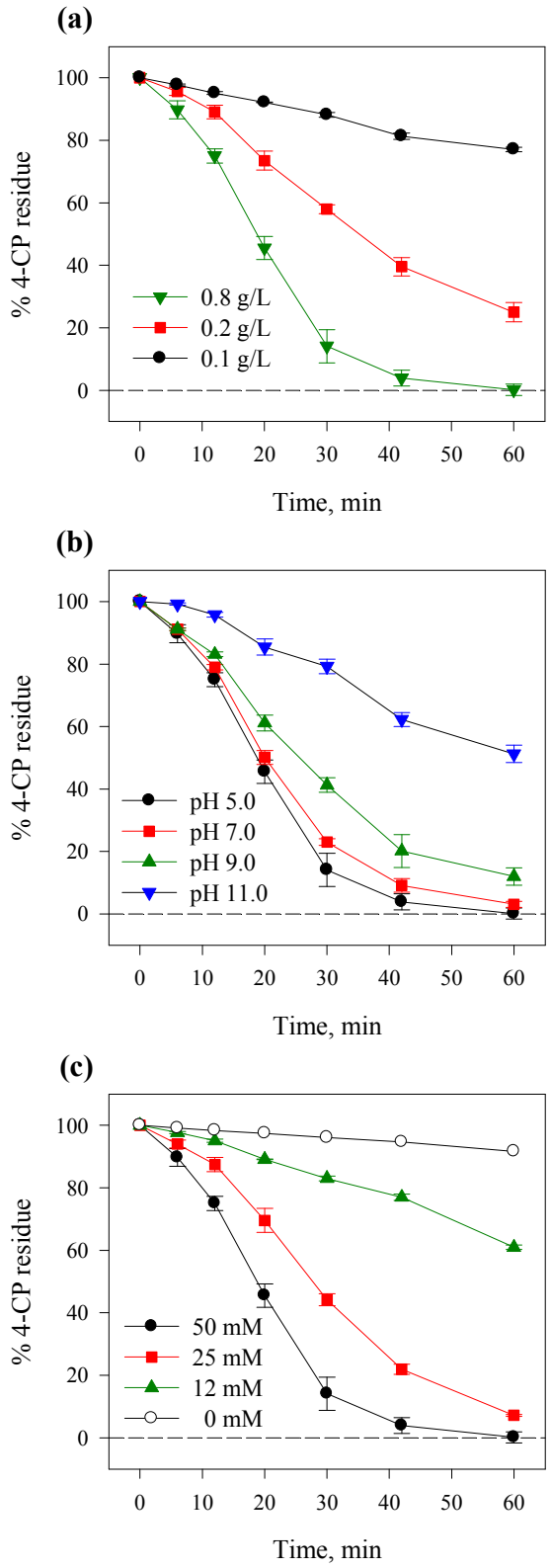

Fig. 5

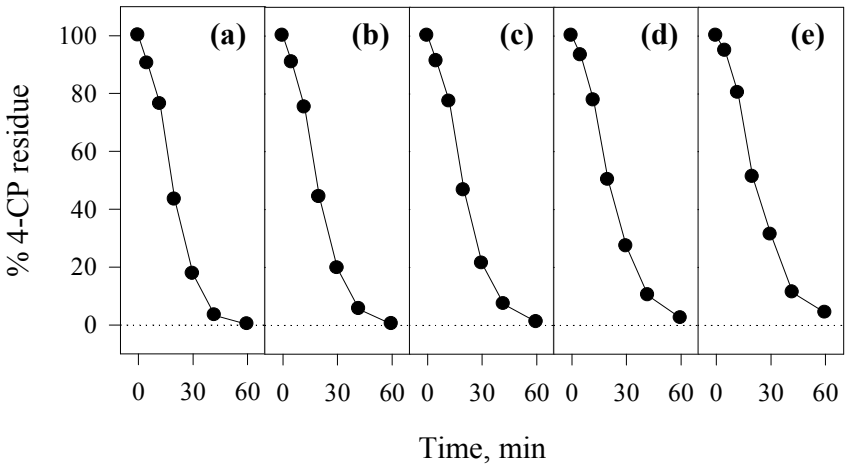

Fig. 6

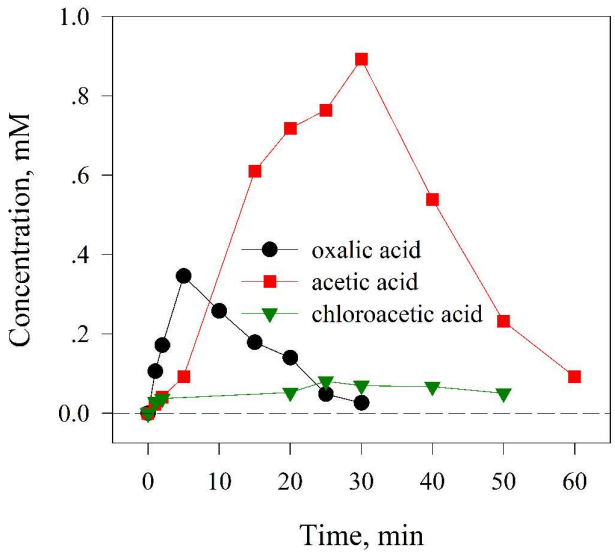

Fig. 7

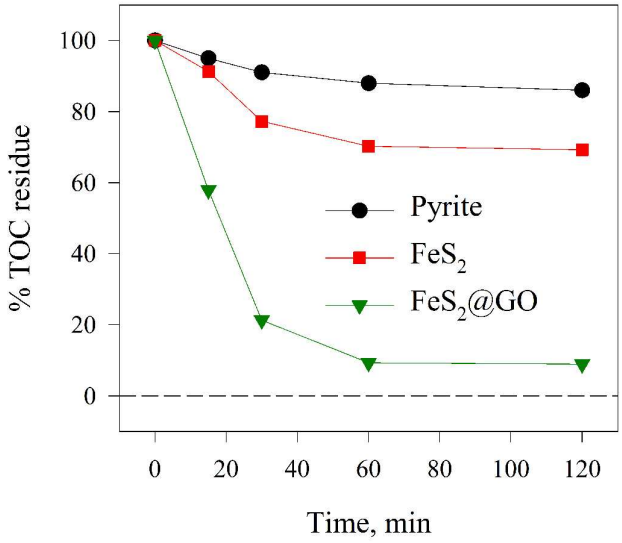

Fig. 8

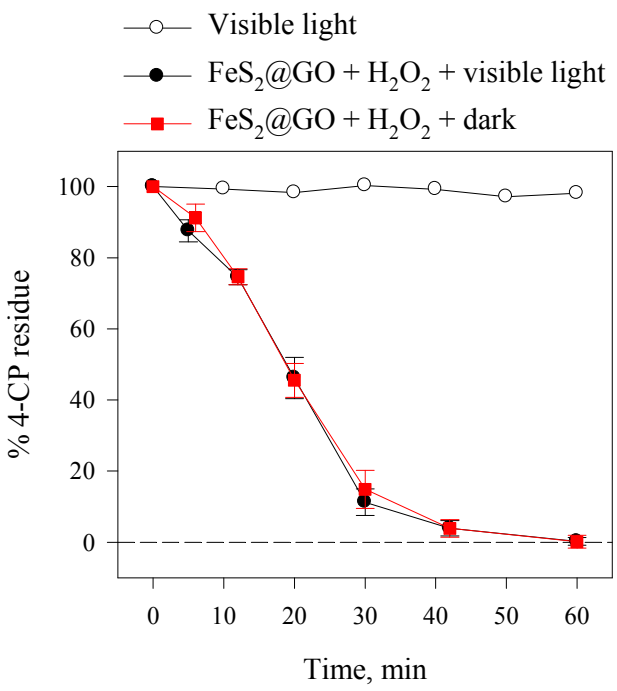

Fig. 9

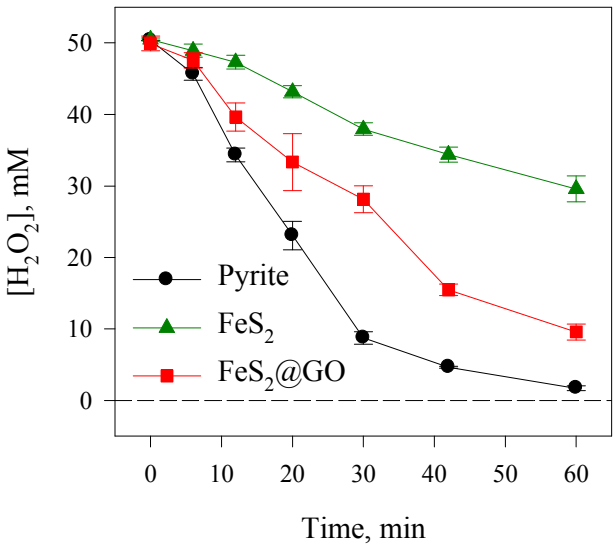

Fig. 10

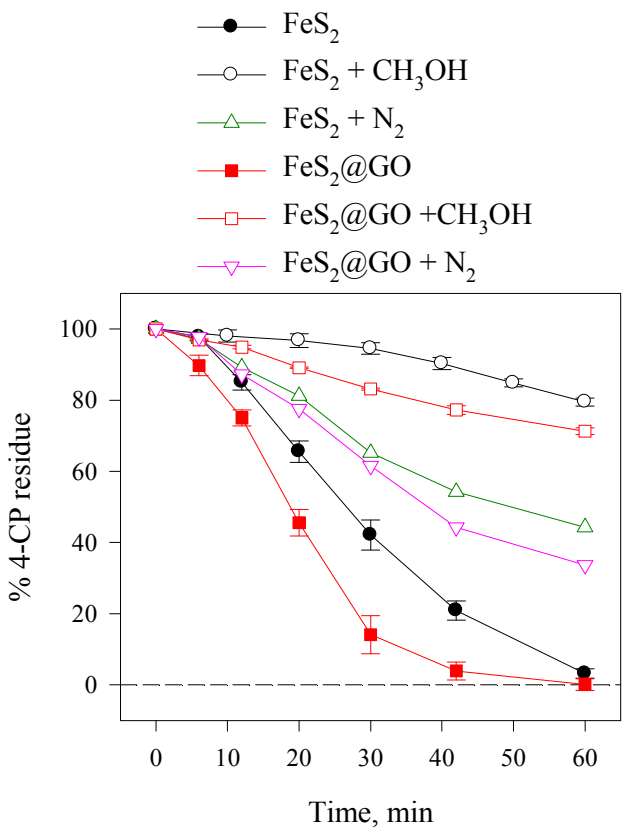

Fig. 11